

Dual-stator Two-phase Permanent Magnet Machines with Phase-group Concentrated-coil Windings for Torque Enhancement

Wenliang Zhao¹, Thomas A. Lipo², *Life Fellow, IEEE*, and Byung-il Kwon¹, *Senior Member, IEEE*

¹Department of Electronic Systems Engineering, Hanyang University, Ansan, 426-791, Korea

²Department of Electrical and Computer Engineering, Florida State University, Tallahassee FL, 32306, USA

This paper presents two types of novel dual-stator, two-phase permanent magnet synchronous machines (PMSMs) equipped with an advanced phase-group concentrated-coil winding and a spoke-type permanent magnet (PM) array for direct-drive applications. The key advantage of the proposed two-phase PMSMs is its superior flux focusing effects, which greatly enhance the torque, benefitting from the whole machine configuration. To highlight the advantages of the proposed two-phase PMSMs, one three-phase PMSM and one two-phase PMSM with conventional stator and winding configurations are adopted for comparison. All relevant machine characteristics, including the airgap flux density, back electromotive force (EMF), and electromagnetic torque are predicted by a two-dimensional (2-D) finite element method (FEM). Finally, one of the proposed dual-stator, two-phase PMSMs is optimized to minimize cogging torque and torque ripple using the Kriging method and a genetic algorithm (GA).

Index Terms—Cogging torque, phase-group concentrated-coil winding, dual-stator, electromotive force (EMF), finite element method (FEM), genetic algorithm (GA), permanent magnet synchronous machines (PMSMs), spoke-type, two-phase.

I. INTRODUCTION

DUE TO the high torque/power density and high efficiency, permanent magnet synchronous machines (PMSMs) have been comprehensively investigated and employed in various industrial, transportation, and renewable energy applications. In general, three-phase PMSMs are the most common choice benefitting from their good utilization of materials and well-known high performance [1]-[2]. However, two-phase PMSMs have become increasingly attractive for low-cost applications because of their relatively low drive system cost and competitive performance in terms of torque density when compared with three-phase PMSMs [3]-[5].

It has been found that two- and three-phase PMSMs with the same slot/pole number combinations can produce similar torque density and efficiency for low-speed applications [3]. In [4], the electromagnetic performance of a two-phase machine with 8 slots and 10 poles and a three-phase machine with 12 slots and 10 poles are compared at 6000 rpm, which shows that the two-phase machine has higher torque density with higher torque ripple than the three-phase machine. In [5], the authors showed that a two-phase drive system without voltage doubling exhibits almost the same power density as a three-phase system under six-state operation. Nevertheless, the reported models for two-phase PMSMs generally adopt the conventional design criteria or techniques resulting in a consequent limited performance improvement. For example, two-phase PMSMs generally utilize concentrated windings to obtain short end turns and winding loss but suffer a low effective winding factor. Hence, the development of novel topologies for two-phase PMSMs with improved performance continues to be a desirable and important topic for the future.

Manuscript received March 20, 2015, revised May 30, 2015, accepted June 14, 2015. Corresponding author: Byung-il Kwon (e-mail: bikwon@hanyang.ac.kr).

Digital Object Identifier inserted by IEEE

In this paper, by taking advantage of a phase-group concentrated-coil winding and a spoke-type PM array [6], two types of novel dual-stator, two-phase PMSMs with significant torque enhancement are proposed for direct-drive applications. To highlight the advantages of the proposed dual-stator two-phase PMSMs, the dual-stator, three-phase and two-phase PMSMs with conventional stator and winding configurations are adopted for comparison based on a 2-D finite element method (FEM) using the commercial software, JMAG-Designer. Finally, one of the proposed dual-stator, two-phase PMSMs is optimized to minimize cogging torque and torque ripple using the Kriging method and a genetic algorithm (GA).

II. TOPOLOGIES OF THE INVESTIGATED MACHINES

A. Machine Topologies

This study outlines a quantitative comparison among the conventional three-phase and two-phase, and the proposed two-phase PMSMs, offering insights into the contributions of the proposed models. The topologies of the machine models are illustrated in Fig. 1. The conventional dual-stator, three-phase and two-phase PMSMs (model 1 and model 2) are shown in Figs. 1(a) and (b), while the proposed dual-stator, two-phase PMSMs (model 3 and model 4) are shown in Figs. 1(c) and (d), respectively. All of the machine models share the same rotor configuration with circumferentially magnetized NdFeB magnets, as shown in Fig. 1(e). The specifications of all the machines are listed in Table I.

The conventional dual-stator, three-phase and two-phase machine models are designed following the typical design criteria as given in [2], featuring uniform stator teeth and slot widths, which are equipped with traditional concentrated windings. In the proposed dual-stator, two-phase machine models, a series of stator teeth are constructed to be in a group with the same phase winding designated as phase-group concentrated-coil windings. The proposed model 3 exhibits a wider slot width, while the proposed model 4 features wider teeth widths between the two different phases.

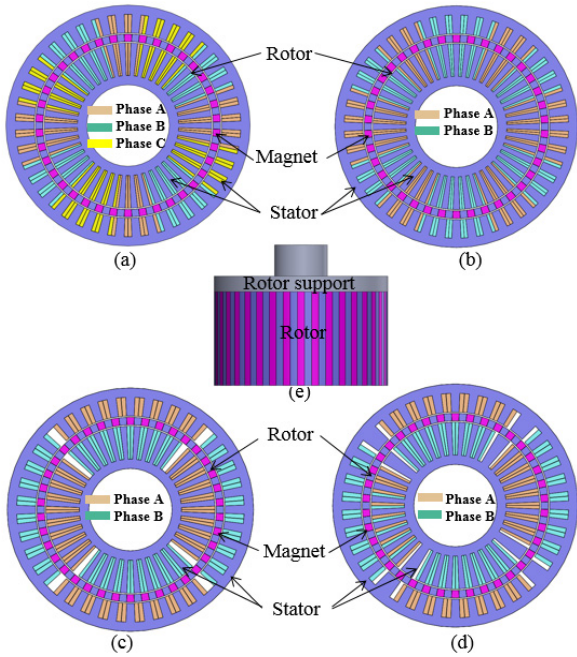


Fig. 1. Machine topologies. (a) Conventional three-phase PMSM (Model 1). (b) Conventional two-phase PMSM (Model 2). (c) Proposed two-phase PMSM-slot (Model 3). (d) Proposed two-phase PMSM-teeth (Model 4). (e) Rotor-PM configuration.

TABLE I
SPECIFICATIONS OF THE INVESTIGATED MACHINES

Item	Unit	Model 1	Model 2	Model 3	Model 4
Phase	-	Three	Two		
Slots/poles	-	42/38	44/38	36/38	
Motor outer diameter	mm	133			
Motor inner diameter	mm	44			
Axial length	mm	60			
Airgap length	mm	0.7			
Remanence of magnet	T	1.16			
Turns per phase	-	266	396	396	400
Phase resistance	Ω	0.742	1.100	1.098	1.104

B. Design Criteria and Operating Principle

The superiority of the proposed two-phase PMSMs is illustrated in Fig. 2. The conventional model 1 and model 2 adopt uniform stator teeth and slot widths with two aligned stators and conventional concentrated windings, in which the PM flux will be distributed into two airgaps as shown in Fig. 2(a). In the proposed model 3 and model 4, the slot and teeth widths within one phase group are designed to be the same as $\pi/2$ radians (electrical), whereas the slot width in model 3 and the teeth width in model 4 between two different phases are π radians (electrical). Furthermore, the two stators in the proposed models are offset by π radians (electrical). Therefore, almost all of the PM flux will be focused into one airgap corresponding to the same phase A or B when the rotor pole rotates to become aligned with the teeth of one of the stators as depicted in Figs. 2(b) and 2(c), respectively. Thus, a higher airgap flux density resulting in a higher resultant torque can be obtained in the proposed two-phase machine models compared to the conventional two-phase and three-phase machine models in which two airgaps work independently.

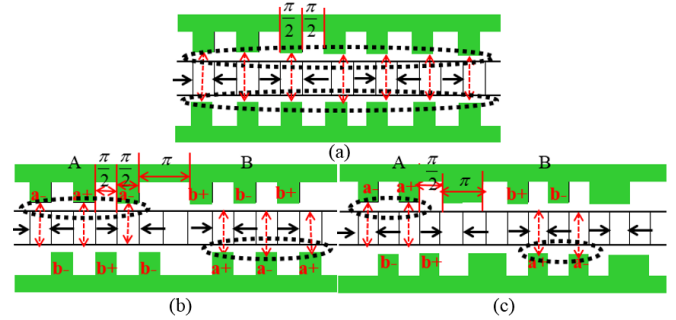


Fig. 2. Design sketch (developed view). (a) Conventional model 1 and model 2. (b) Proposed model 3. (c) Proposed model 4.

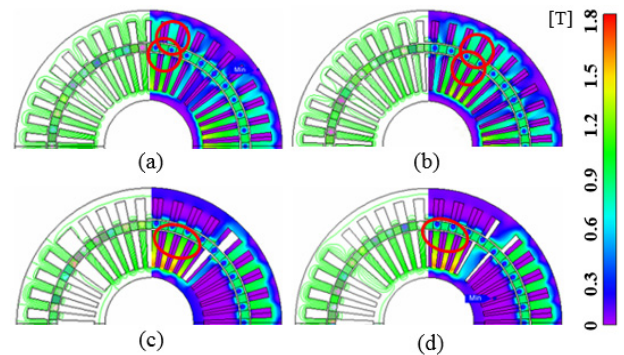


Fig. 3. Magnetic flux density distribution. (a) Conventional model 1. (b) Conventional model 2. (c) Proposed model 3. (d) Proposed model 4.

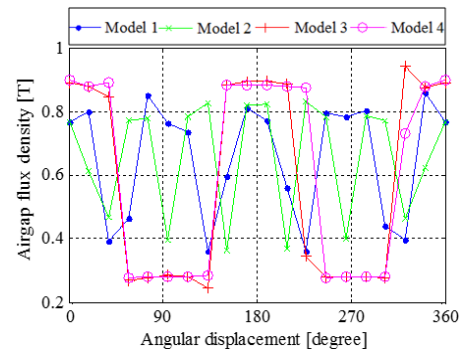


Fig. 4. Comparison of airgap flux density.

III. FEM ANALYSIS RESULTS

A. Magnetic Flux Density and Back EMF

All of the machine characteristics are predicted by a 2-D FEM. The open-circuit magnetic flux density distribution is shown in Fig. 3. As depicted by the operating principle, the PM flux in the conventional models is distributed equally into two airgaps in Figs. 3(a) and (b), while the PM flux of the proposed models is focused into one airgap as shown in Figs. 3(c) and (d), respectively. Hence, a higher airgap flux density is obtained in the proposed model 3 and model 4 than the conventional model 1 and model 2, as demonstrated in Fig. 4.

The comparison of back EMFs in phase is shown in Fig. 5. Fig. 6 shows the corresponding fast Fourier transform (FFT) analysis. Both of the proposed two-phase machine models have increased fundamental and rms values of back EMFs in phase, although they exhibit higher harmonics than the conventional three-phase and two-phase machine models.

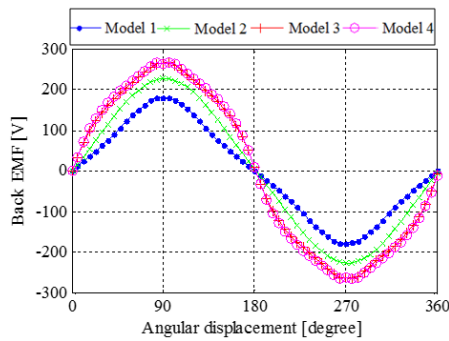


Fig. 5. Comparison of back EMFs in phase.

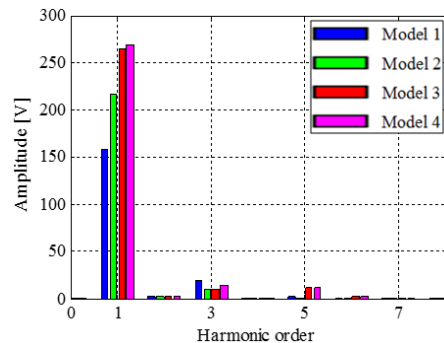


Fig. 6. FFT analysis of back EMFs in phase.

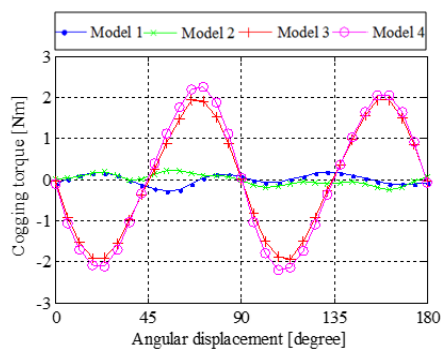


Fig. 7. Comparison of cogging torques.

B. Torque Characteristics

Fig. 7 shows the comparison of cogging torques. It shows that the cogging torques in the proposed models 3 and 4 are substantially increased, due to the improved airgap flux density which is revealed in Fig. 4, as a result of the superior flux focusing effects benefiting from the proposed operating principle. The electromagnetic torques, obtained by feeding the stator windings with sinusoidal current excitations at a current density of 5.5 Arms/mm^2 , are compared in Fig. 8. The average torques in both of the proposed models increase significantly, by more than 10.8% and 21.4%, compared to those of the conventional models 1 and 2, respectively. Accordingly, the torque density and efficiency as estimated in [6] of the proposed models are also improved, as listed in Table II. However, the torque ripple in the proposed models, which is the ratio of the peak-to-peak torque value to the average torque value, is higher than that of the conventional models. In general, such torque ripple, together with the cogging torque, is unacceptable for many applications and therefore must be minimized as shown in the next section.

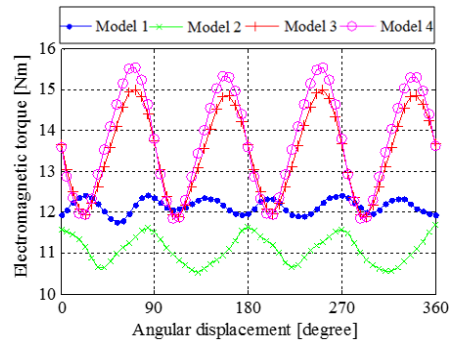


Fig. 8. Comparison of electromagnetic torques.

TABLE II
2-D FEM ANALYSIS RESULTS

Item	Unit	Model 1	Model 2	Model 3	Model 4
Back EMF	V	113	154	187	191
Cogging torque	Nm	0.4798	0.4879	3.9894	4.5205
Torque	Nm	12.15	11.09	13.46	13.72
Torque density	Nm/L	14.63	13.36	16.21	16.53
Torque ripple	%	5.55	10.54	23.27	27.54
Power @750rpm	W	954.41	871.18	1057.7	1077.6
Copper loss	W	35.61	35.18	35.12	35.32
Iron loss	W	55.69	54.67	58.41	55.88
Efficiency	%	91.07	90.52	92.09	92.27

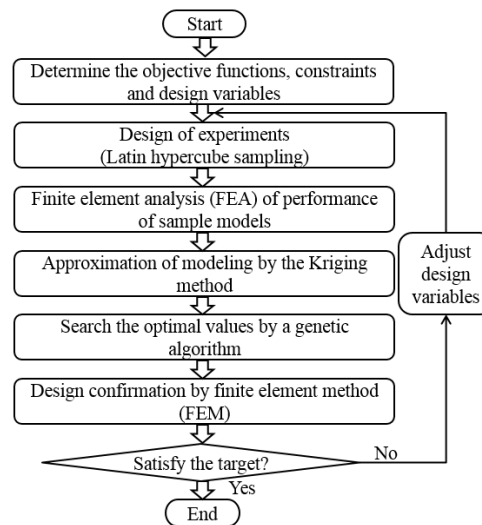


Fig. 9. Optimal design process.

IV. OPTIMIZATION

The proposed model 3 has been selected for purposes of optimization to minimize cogging torque and torque ripple. Fig. 9 depicts the optimal design process. First, the objective functions, constraints, and design variables are determined. Then, Latin hypercube sampling is applied in a design of experiments process in order to select the sampling points, and the Kriging method is performed for approximation modeling. Using a GA, the optimal points for the design variables are obtained. Finally, the optimal design results are verified by utilizing 2-D FEM.

The objective functions for minimizing cogging torque and torque ripple are shown in (1), which will be carried out by assigning the weighting values to each objective function [7],

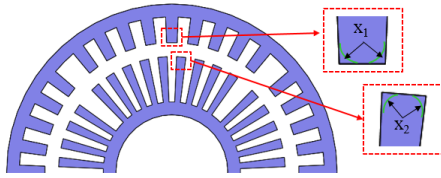


Fig. 10. Design variables of the proposed model 3.

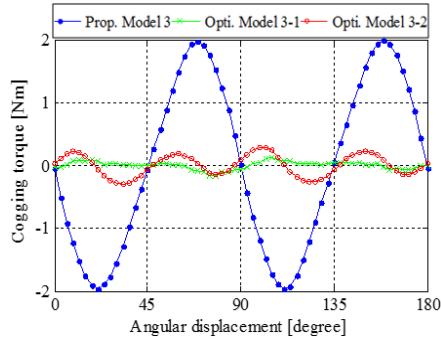


Fig. 11. Cogging torques of the proposed and optimized model 3.

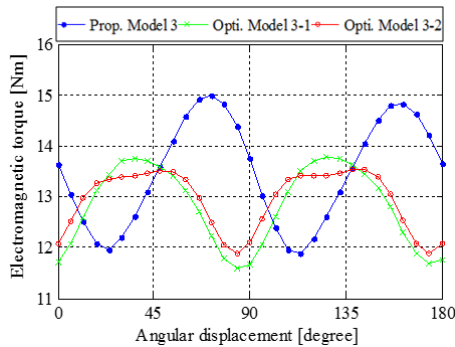


Fig. 12. Electromagnetic torques of the proposed and optimized model 3.

utilizing the commercial optimization tool, PIA^{no} [8]. The constraints are set to prevent torque and efficiency from severe degradation as shown in (2). The design variables are selected as the arc radius of the stator teeth ends, designated as x_1 (outer stator) and x_2 (inner stator) as shown in Fig. 10 and (3).

- *Objective functions:*
Minimizing cogging torque and torque ripple (1)
- *Constraints:*
Electromagnetic torque > 12.74 Nm
Efficiency $> 91.15\%$ (2)
- *Design variables:*
 $0.8 \text{ mm} \leq x_1 \leq 1.6 \text{ mm}$
 $0.5 \text{ mm} \leq x_2 \leq 1.4 \text{ mm}$ (3)

The optimal design variables obtained from two weighting setups of the objective functions are listed in Table III. Fig. 11 and Fig. 12 show the comparison of cogging torques and electromagnetic torques, respectively. Compared to the proposed model 3 (M3), the cogging torque and torque ripple of the optimized model 3 in both weighting-setup cases (M3-1 and M3-2) are significantly reduced, as also indicated by the data in Table III. It is worthy to note here that the torque ripple in the optimized models is just suppressed to be a general but not superior level due to the relatively high total harmonics distortion (THD) in back EMFs as listed in Table III.

TABLE III
OPTIMIZATION RESULTS OF THE PROPOSED MODEL 3

Item	Unit	Prop. M3	Opti. M3-1	Opti. M3-2
Weighting*	-	-	0.5/0.5	0.3/0.7
x_1	mm	-	1.0	0.9
x_2	mm	-	0.83	0.85
Cogging torque	Nm	3.9894	0.3046	0.5899
THD in back EMF	%	6.1	8.9	7.5
Torque	Nm	13.46	12.85	12.96
Torque ripple	%	23.27	17.05	12.75
Efficiency	%	92.09	91.95	91.98

* The weighting is expressed by the form as cogging torque/torque ripple.

V. CONCLUSION

This paper has proposed two types of novel dual-stator, two-phase PMSMs to improve torque performance by utilizing of a phase-group concentrated-coil winding, a spoke-type PM array, and two unaligned stators. Through a comparison with the conventional three- and two-phase PMSMs, it has been demonstrated that both of the proposed models exhibit greatly enhanced torque based on the 2-D FEM analysis results. Optimization using the Kriging method and a GA is shown to substantially minimize cogging torque and torque ripple of the proposed models. Hence, the proposed dual-stator, two-phase PMSMs could be attractive alternatives for direct-drive applications in which high torque performance is required.

ACKNOWLEDGMENT

This research was jointly supported by the BK21PLUS program through the National Research Foundation of Korea funded by the Ministry of Education, and the Human Resources Program in Energy Technology of the Korea Institute of Energy Technology Evaluation and Planning (KETEP), granted financial resource from the Ministry of Trade, Industry and Energy, Republic of Korea (20154030200730).

REFERENCES

- [1] N. Bianchi, S. Bolognani, and E. Fornasiero, "An overview of rotor losses determination in three-phase fractional-slot PM machines," *IEEE Trans. Ind. Appl.*, vol. 46, no. 6, pp. 2338-2345, Nov./Dec. 2010.
- [2] J. R. Hendershot, and T. J. E. Miller, *Design of Brushless Permanent Magnet Machines*, 2nd ed., Motor design books LLC, 2010, pp. 71-152.
- [3] K. Wang, Z. Q. Zhu, L. J. Wu, and G. Ombach, "Comparison of electromagnetic performance of 2- and 3-phase PM brushless AC machines for low speed applications," *Power Electronics, Machines and Drives (PEMD 2012)*, Mar. 27-29, 2012, pp. 1-6.
- [4] J. Chai, J. B. Wang, K. Atallah, and D. Howe, "Performance comparison and winding fault detection of duplex 2-phase and 3-phase fault-tolerant permanent magnet brushless machines," in *42nd IEEE IAS Annual Meeting Conf. Record*, Sep. 23-27, 2007, pp. 566-572.
- [5] Y. Li, T. A. Walls, J. D. Lloyd, and J. L. Skinner, "A novel two-phase BPM drive system with high power density and low cost," *IEEE Trans. Ind. Appl.*, vol. 34, no. 5, pp. 1072-1080, Sep./Oct., 1998.
- [6] W. Zhao, T. A. Lipo, and B. I. Kwon, "Comparative study on novel dual stator radial flux and axial flux permanent magnet motors with ferrite magnets for traction application," *IEEE Trans. Magn.*, vol. 50, no. 11, p. 8104404, Nov. 2014.
- [7] K. C. Kim, J. Lee, H. J. Kim, and D. H. Koo, "Multiobjective optimal design for interior permanent magnet synchronous motor," *IEEE Trans. Magn.*, vol. 45, no. 3, pp. 1780-1783, Mar. 2009.
- [8] PIA^{no} introduction: <http://www.pidotech.com/en/product/piano2.aspx>.